Title

THE FATIGUE CRACK GROWTH BEHAVIOR IN A NITROGEN-STRENGTHENED HIGH-MANGANESE STEEL AT CRYOGENIC TEMPERATURES

Author

Morris, J.W.

Publication Date

1983-05-01

Lawrence Berkeley Laboratory
UNIVERSITY OF CALIFORNIA

Materials & Molecular Research Division

Presented at The Metallurgical Society Symposium on Fatigue at Low Temperatures, Louisville, KY, May 10, 1983

THE FATIGUE CRACK GROWTH BEHAVIOR IN A NITROGEN-STRENGTHENED HIGH-MANGANESE STEEL AT CRYOGENIC TEMPERATURES

R. Ogawa and J.W. Morris, Jr.

May 1983

Prepared for the U.S. Department of Energy under Contract DE-AC03-76SF00098

DISCLAIMER

THE FATIGUE CRACK GROWTH BEHAVIOR IN A NITROGEN-STRENGTHENED HIGH-MANGANESE STEEL AT CRYOGENIC TEMPERATURES

By

R. Ogawa* and J. W. Morris, Jr.

Department of Materials Science and Mineral Engineering
and
Lawrence Berkeley Laboratory

University of California, Berkeley

ABSTRACT

The fatigue crack growth rate (FCGR) of a nitrogen-strengthened high manganese stainless steel of nominal composition 18Mn-5Ni-16Cr-0.02C-0.22N was determined in the intermediate stress-intensity factor range (20-70 MPa m) at 77K and 4K. Fractographic investigations were performed on the fracture surfaces. The FCGR at 4K is very nearly the same as that at 77K and substantially below the crack growth rate for AISI 304LN steel. The fracture surfaces of both the high-manganese alloy and the 304LN showed a transgranular failure mode, but the detailed fractographic features varied with temperature and alloy type. The fractography was closely related to changes in the FCGR.

KEY WORDS: Fatigue crack growth rates, FCGR, nitrogen-strengthened high manganese steel, 18Mn-5Ni-16Cr-0.02C-0.22N, intermediate stress intensity factor range, cryogenic temperatures, transgranular failure mode.

* On leave from Kobe Steel, Ltd., Kobe, Japan.

INTRODUCTION

AISI 304L and 316L stainless steels are common cryogenic alloys that have been widely used for 4K service. They show excellent ductility and toughness at cryogenic temperatures but have relatively low yield strength. The recent development of large superconducting magnets, especially for fusion reactors, has created new needs for high strength structural alloys. Nitrogen-strengthened stainless steels such as AISI 304LN and 316LN were used for the cases of the toroidal field coil for the Large Coil Project for fusion reactor research [1]. However, much higher strength steels will be required for the next step test facility because of planned increases in the size and electromagnetic force of the toroidal field coils. These new materials must also have good fatigue resistance since the toroidal field coils will be exposed to cyclic forces from the poloidal field coils [1].

Fatigue crack growth rates (FCGR) were measured in several austenitic stainless steels at cryogenic temperatures by Reed, et al. [2] and Tobler, et al. [3]. Tobler has shown that the FCGR of the 304 stainless steels is increased at cryogenic temperatures by the addition of interstitial carbon and nitrogen, and they also discussed the effect of the stability of the austenite phase on the FCGR. However, the role of the strain-induced transformation (stability of austenite) remains unclear because both the stable 310 type stainless steel and the least stable 304L steel show superior fatigue crack resistance at cryogenic temperatures [3].

In order to satisfy the need for new cryogenic structural alloys, a number of new high manganese austenitic steels have been developed. These alloys offer low cost, stable austenite and high strength. Previous research [4] has shown that promising cryogenic properties can be obtained in a modified 200 series high manganese stainless steel having nominal alloy composition 18Mn-5Ni-16Cr-0.02C-0.22N. The present study was undertaken to evaluate the fatigue crack propagation behavior of this alloy at cryogenic temperatures.

EXPERIMENTAL WORK

A 300 kg ingot of nominal composition 18Mn-5Ni-16Cr-0.02C-0.22N was prepared by vacuum-induction melting. The ingot was hot-forged to 80mm thickness plate and then hot-rolled at 1523K to 30mm thickness plate. One part of the plate was solution-treated at 1323K for 1.8 ks followed by water quenching. Compact tension (CT) specimens were cut from the center of the thickness of the hot-rolled and solution-treated plates. AISI 304LN steel plate of 76.2mm thickness was used to compare the fatigue crack propagation behavior. CT specimens were prepared from plates of this alloy in the as-rolled condition. The measured alloy compositions are given in Table 1.

The compact tension specimen dimensions were w=50.8mm and B=25.4mm (B=23.2mm for 304LN). The original mechanical notch length was an-15.88mm and the direction of the notch was perpendicular to the plate rolling direction (LT orientation). The fatigue tests were carried out using an Instron servo-hydraulic machine and cryostat. The tests were run at 10 Hz in load control (R=0.125) using a sinusoidal tension stress

wave form. The crack length was measured from the sample compliance. The fatigue crack growth rates (da/dN) were obtained for intermediate ΔK (20-70 MPa $\sqrt{m}$). After testing, the fatigued specimens were broken or cut into two halves. The fracture surfaces were investigated by scanning electron microscopy. The fatigue crack paths were studied in an optical microscope using either unbroken specimens or broken specimens whose fracture surfaces were plated with Ni.

RESULTS AND DISCUSSION

Cryogenic Mechanical Properties.

The tensile and Charpy impact properties of 18Mn-5Ni-16Cr-0.02C-0.22N alloy are listed in Table 2. The yield (0.2% flow stress) and tensile strengths increase significantly as the deformation temperature is lowered from 293 to 77 and 4K. The total elongation decreases as the temperature is lowered but remains over 35% at 4K. The as-rolled plate has higher strength and ductility at 4K than the solution-treated plate. The Charpy V-notch absorption energies decrease at cryogenic temperatures to approximately half their values at room temperature, but the absorbed energies at 4K are comparable to those at 77K and ductile dimple fracture surfaces are observed. The alloys were metastable to transformation to either the ε or α' martensite phase during low temperature deformation. Approximately 34% ε phase and 6% of α' phase were found in the solution-treated tensile specimen after it had been broken at 4K. The specimen deformed by 17% at 4K showed 17% ε phase and 0% α phase. Comparing the high-manganese alloy to the 30L and 304LN alloys, the austenite phase in this alloy is relatively unstable with respect to the $\gamma \rightarrow \varepsilon$ transformation during low-temperature deformation, but it is relatively stable with respect to the $\gamma \rightarrow \alpha'$ (or $\gamma \rightarrow \alpha \rightarrow \alpha'$) transformation [3].

Fatigue Crack Growth Rates (FCGR).

The fatigue crack growth rate of the experimental alloy is plotted as a function of Δ at 77K and 4K in Figure 1. Both the data previously reported and that obtained in the present work are included for the 304LN steels. The data obey the Paris equation:

$$da/dN = C\ (\Delta)^n \qquad (1)$$

where C and n are constants that depend on material and temperature. The values of C and n obtained from the data in Figure 1 are given in Table 3.

The FCGR of the experimental alloy in both the as-rolled and solution-treated conditions is substantially below that of 304LN steel and slightly higher than that reported for 304 and 304L steels. The experimental alloy also differs from 304LN in the temperature dependence of the fatigue crack growth rate. While 304LN exhibits a substantial increase in its FCGR as the temperature is reduced from 77K to 4K, the fatigue crack growth rates in the experimental alloy are nearly the same at the two temperatures. The FCGR of the experimental alloy is slightly dependent on its heat treatment. The FCGR in the as-rolled plate is slightly below that of the solution-treated plate, and it increases somewhat when the temperature is decreased from 77K to 4K. The solution-

treated plate exhibits a change in the slope of the Paris curve when the temperature is lowered to 4K (n=2.8 to 4.2). As a consequence of the slope change, the FCGR curves cross: for ΔK less than bout 50 MPa $m^{1/2}$ the FCGR at 4K is less than that at 77K.

Metallography.

Both optical and scanning electron fractography show that the fracture path in the experimental alloy is transgranular at 77K for both the as-rolled and solution-treated conditions. Scanning electron fractographs of the 77K fracture surfaces are shown in Figure 2. The direction of crack propagation varies from grain to grain and sometimes changes within a grain. Well-defined striations and microcracks are visible on the fracture surface of the as-rolled plate (Fig. 2a). These are oriented almost perpendicular to the direction of the crack propagation. The striations are poorly defined on the fracture surface of the solution-treated plate (Fig. 2b). They are feather-like and oriented differently in each grain.

The failure mode of the 304LN steel was also completely transgranular at 77K. The direction of crack propagation was again found to change at the grain boundaries and occasionally inside the grains, but the fracture surface was flatter than in the experimental alloy (Fig. 3a). Each exposed facet exhibits a fine microstructure that is associated with the transformed martensite (Fig. 3b). The α' martensite could be detected on the fracture surfaces of the 304LN steel with a Magnegage, though α' martensite was not detected on the fracture surfaces of the experimental alloy.

Both optical and scanning electron fractography of the fracture surface of the experimental alloy broken at 4K showed that the fracture was again transgranular. The crack propagation path in the as-rolled plate is shown in the optical micrograph given in Figure 4. Many branches (secondary cracks) were seen in the intermediate and high ΔK range. The 4K fracture surface is shown at higher magnification in the scanning electron fractograph given in Figure 5. The fracture surface of the as-rolled plate contains granular facets having feather-like striations that are oriented differently in each grain, together with slip markings and secondary cracks. The typical ductile striations that are seen on the fracture surfaces at 77K disappear at 4K.

The fracture surfaces of the solution-treated plate also show characteristic features. On the portion of the fracture surface that was created in the low ΔK range, some exposed grain facets exhibit striations that are oriented perpendicular to the crack propagation direction, but do not cross the grain. On the surface created at the intermediate and high ΔK range, very smooth grain facets are exposed (Fig. 5d). These may be due to intergranular failure. Crystallographic twins are also occasionally seen.

A typical transgranular failure mode was also observed in 304LN steel after fatigue cracking at 4K (Fig. 6). However, the fracture surfaces differ qualitatively from those on the experimental alloy. Each grain facet displays a fine lamellar structure that reflects the strain-induced martensite transformation, as shown in Figure 7. However, the

lamellar structure is not as clearly defined on the 4K specimen as it is on the surfaces of samples fatigued at 77K.

The above metallographic investigation shows that the change in the FCGR of the experimental alloy with the testing temperature is closely related to the fractographic features on the fracture surface. The as-rolled plate, which has a low FCGR at 77K, displays fine striations that are typical of most ductile metals. This kind of striation is ill-defined on the 4K fracture surface, and the FCGR is slightly higher at this temperature. The solution-treated plate is characterized by the increased slope of the logarithmic FCGR at 4K, and the crossover between the fatigue crack growth rates at 4K and 77K. The change in slope is coincident with a change in the fracture surface morphology. In the low ΔK range where the FCGR at 4K is lower than that at 77K, the grain facets exhibit ductile striations, while in the high ΔK range intergranular and twin-like facets are common. The similarity between the FCGR of the as-rolled plate at 4K and that of the solution-treated plate at 77K is also reasonable in light of the fractography—the two fracture surfaces show similar features.

Fatigue cracks in the experimental alloy propagate mainly along slip planes. Figure 8a shows examples of the crack path trace analysis using the slip markings. Each segment of the zigzag crack is almost parallel to a slip line marking. Fatigue cracks are also found to grow along the slip planes in the initial stages of fatigue crack propagation in ductile metals (Stage I in Reference 5) but follow general planes at higher stress intensities (Stage II). The present alloy is interesting in that it shows crystallographic features in cryogenic fatigue in the Stage II as well.

Crystallographic crack growth was also found in 304LN steel after fatigue cracking at 4K. Figure 8b shows an example of the 4K crack trace of 304LN steel. The local fracture surface was identified as a (110) plane. As the fracture surface at 77K show non-crystallographic features, the increase in the FCGR at 4K might be attributed to the crystallographic crack growth on the {110} plane. Crystallographic fractures have been observed in some aluminum alloys, in which case the fracture surface is (100) or (110) [6,7]. Crystallographic crack growth in aluminum alloys is believed to be enhanced by environmental contaminants that promote brittle fracture on the (110) plane [7]. In the present case, however, it is likely that the crystallographic fracture is associated with the transformation to α' martensite. Although α' martensite is observed on the exposed grain facets at both 77K and 4K, the α' martensite is almost certainly more brittle at 4K than it is at 77K. Brittle α' martensite might enhance the {110} crystallographic crack growth of the matrix.

CONCLUSIONS

A nitrogen-strengthened high manganese steel of nominal composition 18Mn-5Ni-16Cr-0.02C-0.22N showed promising fatigue resistance when compared with 304Ln steel at cryogenic temperatures. The results include:

(1) The FCGR at 4K is almost the same as that at 77K and is substantially below the FCGR of 304LN steel at 4K.

(2) The failure mode was transgranular in both the research alloy and in 304LN at 77K and 4K. Both alloys exhibited a pronounced crystallographic fracture under some conditions, which differs from that previously reported in structural steels in that it occurs in region II of the crack growth behavior.

(3) There is a reasonable correspondence between the fatigue crack growth behavior and the microstructural mechanisms of crack growth, as revealed by fractographic studies of the fatigue surface.

ACKNOWLEDGMENTS

The alloys studied here were supplied by Kobe Steel, Ltd., Kobe, Japan. This research was supported by the Director, Office of Energy Research, Office of Development and Technology, Magnetic Systems Division of the U.S. Department of Energy under contract#DE-AC03-76SF00098.

REFERENCES

1. K. Yoshida, K. Koizumi, H. Nakajima, M. Shimada, Y. Sanada, Y. Takahashi, E. Tada, H. Tsuji and S. Shimamoto: **Proc. of ICMC**, Kobe, Japan, May 11-14, 1982, p. 417.

2. D.T. Reed and R.P. Reed: Materials Studies for Magnetic Fusion Energy Applications at Low Temperatures-II, NBSIR79-1609, National Bureau of Standards, Boulder, COLO, 1979, p.81.

3. R. L. Tobler, D.T. Reed and R.P. Reed: Materials Studies for Magnetic Fusion Energy Applications at Low Temperatures-IV, NBSIR81-1645, National Bureau of Standards, Boulder, COLO, 1981, p.37.

4. R. Ogawa and J.W. Morris, Jr.: **Proc. of ICMC**, Kobe, Japan, May 11-14, 1982, p. 124.

5. P.J.E. Forsyth: Acta metall., 11, 1963, p. 703.

6. G.G. Garrett and J.F. Knott: Acta metall., 23, 1976, p. 841.

7. K.J. Nix and H.M. Flower: Acta metall., 30, 1982, p. 1549.

TABLE 1. Alloy compositions (wt.pct.).

Type	Mn	Ni	Cr	Si	P	S	C	N	C+N
18Mn-5Ni-16Cr	17.98	4.96	16.26	0.53	0.004	0.010	0.024	0.216	0.240
304LN	1.77	9.55	18.54	0.78	0.014	0.009	0.021	0.021	0.160

TABLE 2. Tensile and Charpy impact properties.

Specimen		YS MPa	TS MPa	El.%*	Charpy Impact Values J
As-rolled	293K	323	662	74	300
	77K	855	1319	54	174
	4K	1144	1565	44	170
Solution Treatment	293K	338	656	81	302
	77K	863	1298	64	168
	4K	1074	1556	39	154

* gauge length = 20mm

TABLE 3. Paris equation parameters.

Specimen		n	C	ΔK Region
As-rolled	77K	2.71	9.8×10^{-9}	30~50 MPa $\sqrt{m}$
	4K	3.16	1.95×10^{-9}	35~64
Solution Treatment	77K	2.77	8.03 x 10-9	30~63
	4K	4.18	3.98 x 10-11	30~70

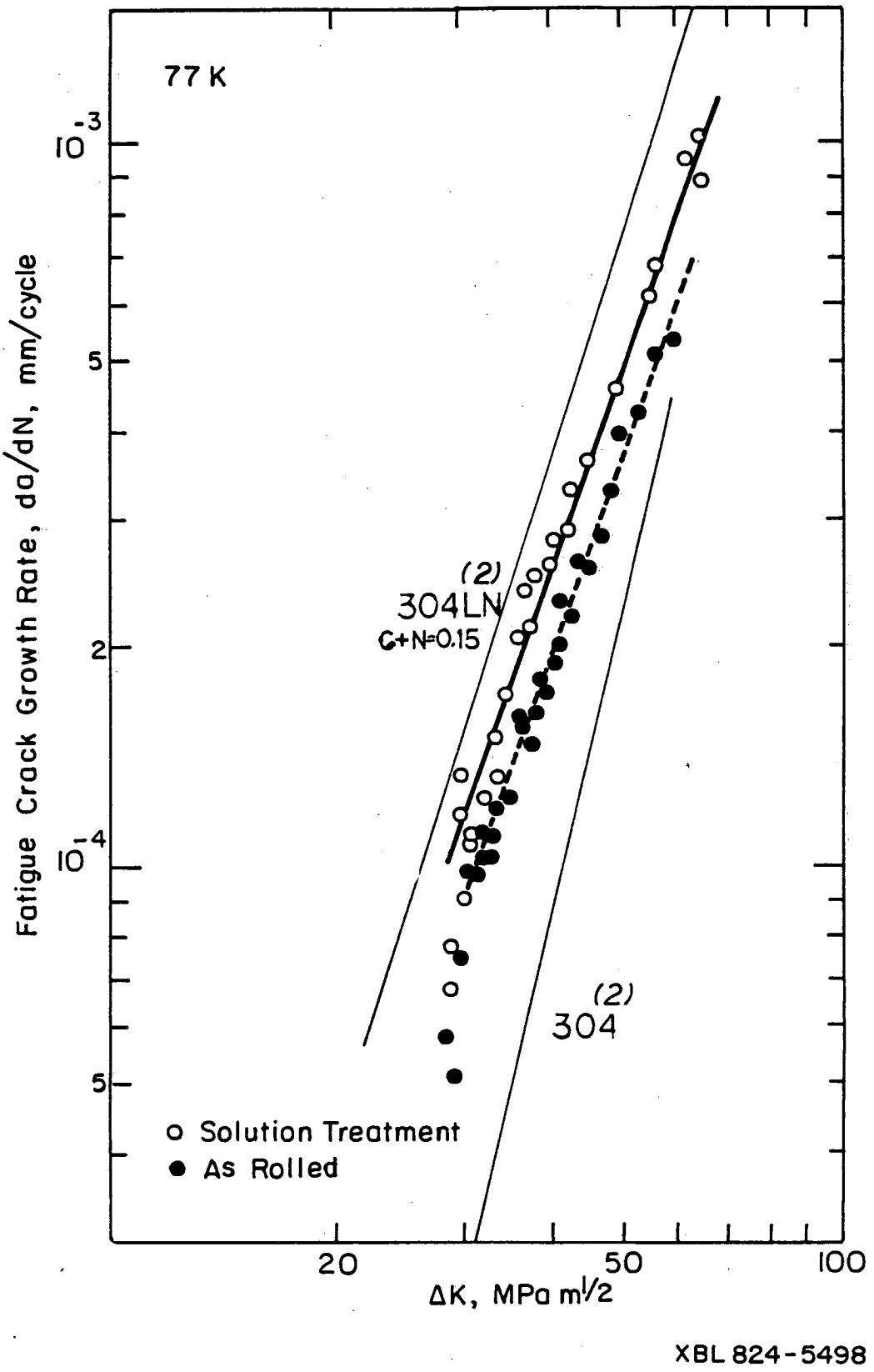

Figure 1a. Fatigue crack growth rates as a function of stress intensity range for 18Mn-5Ni-16Cr-0.01C-0.22N alloy at 77K.

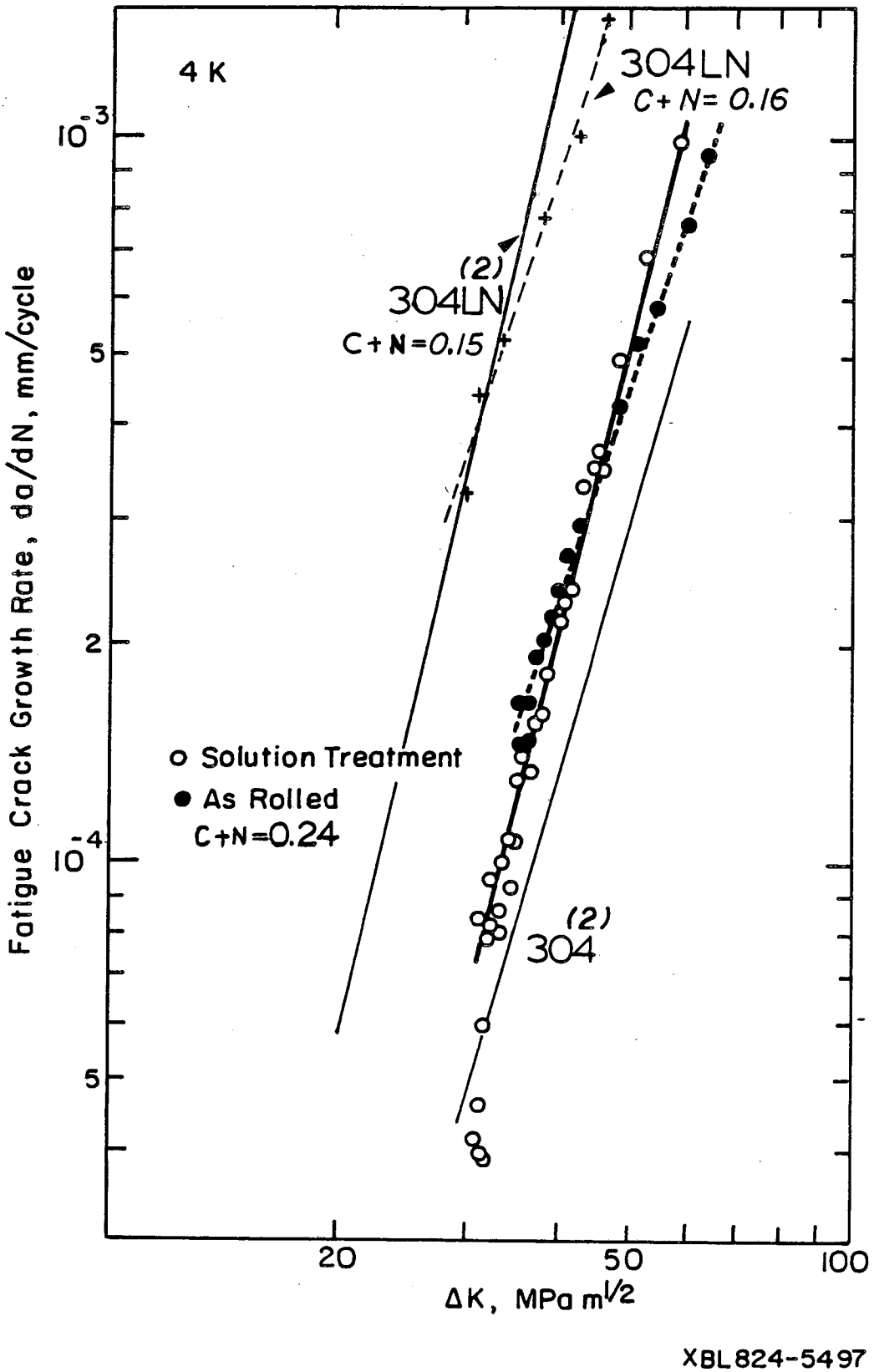

Figure 1b. Fatigue crack growth rates as a function of stress intensity range for 18Mn-5Ni-16Cr-0.01C-0.22N alloy at 4K.

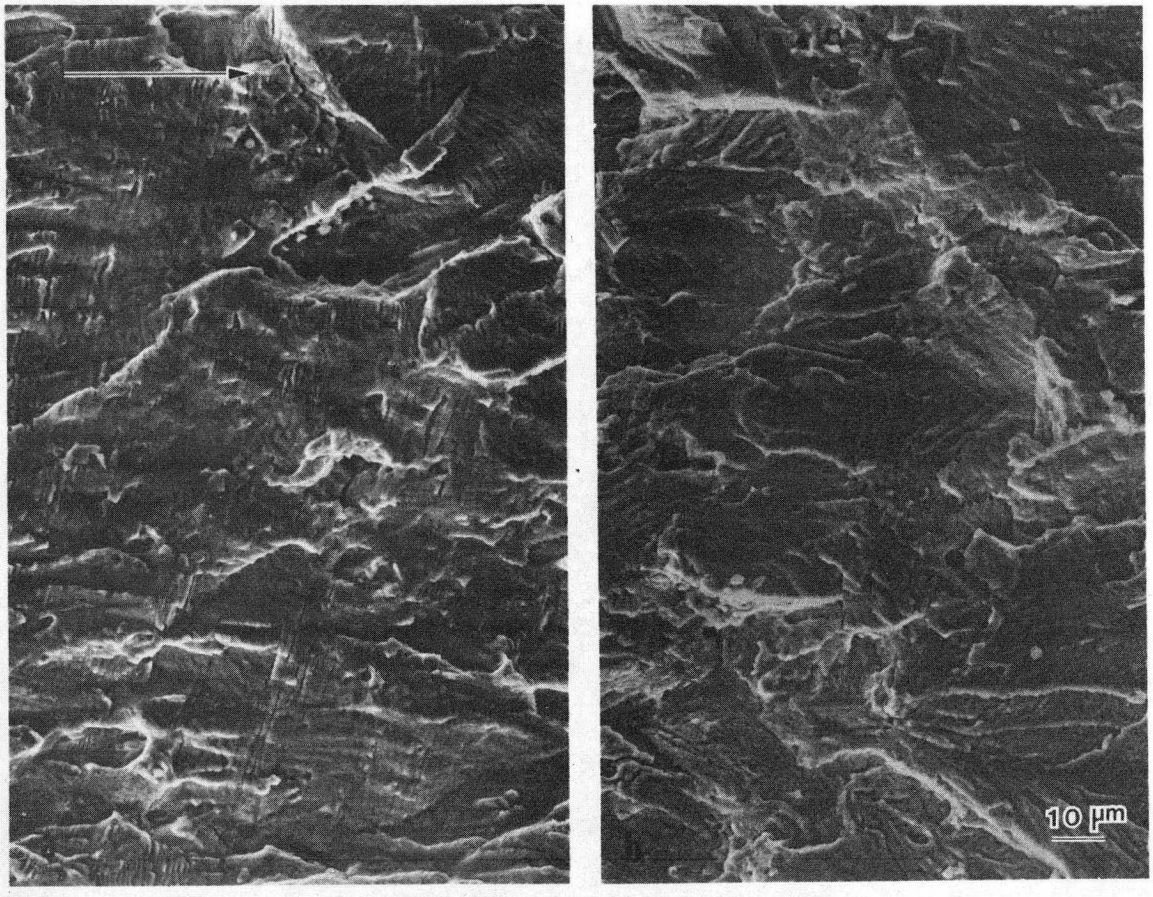

XBB 833-2688

Figure 2. Fracture surfaces after fatigue cracking at 77K. a) as-rolled, b) solution treatment $\Delta K \sim 35$ MPa m.

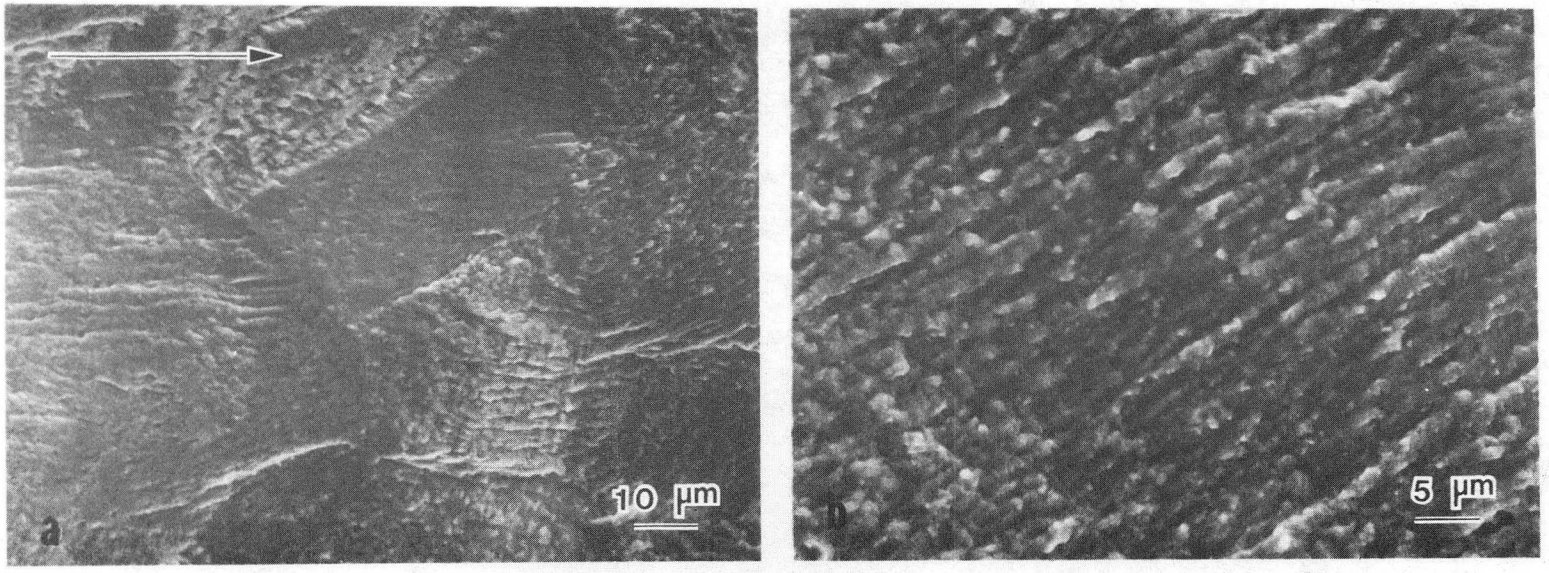

XBB 834-3546

Figure 3. Fracture surface of 304LN steel after fatigue cracking at 77K. a) typical fracture feature, b) fracture lamellae that are associated with the transformed martensite, $\Delta \sim 35$ MPa m.

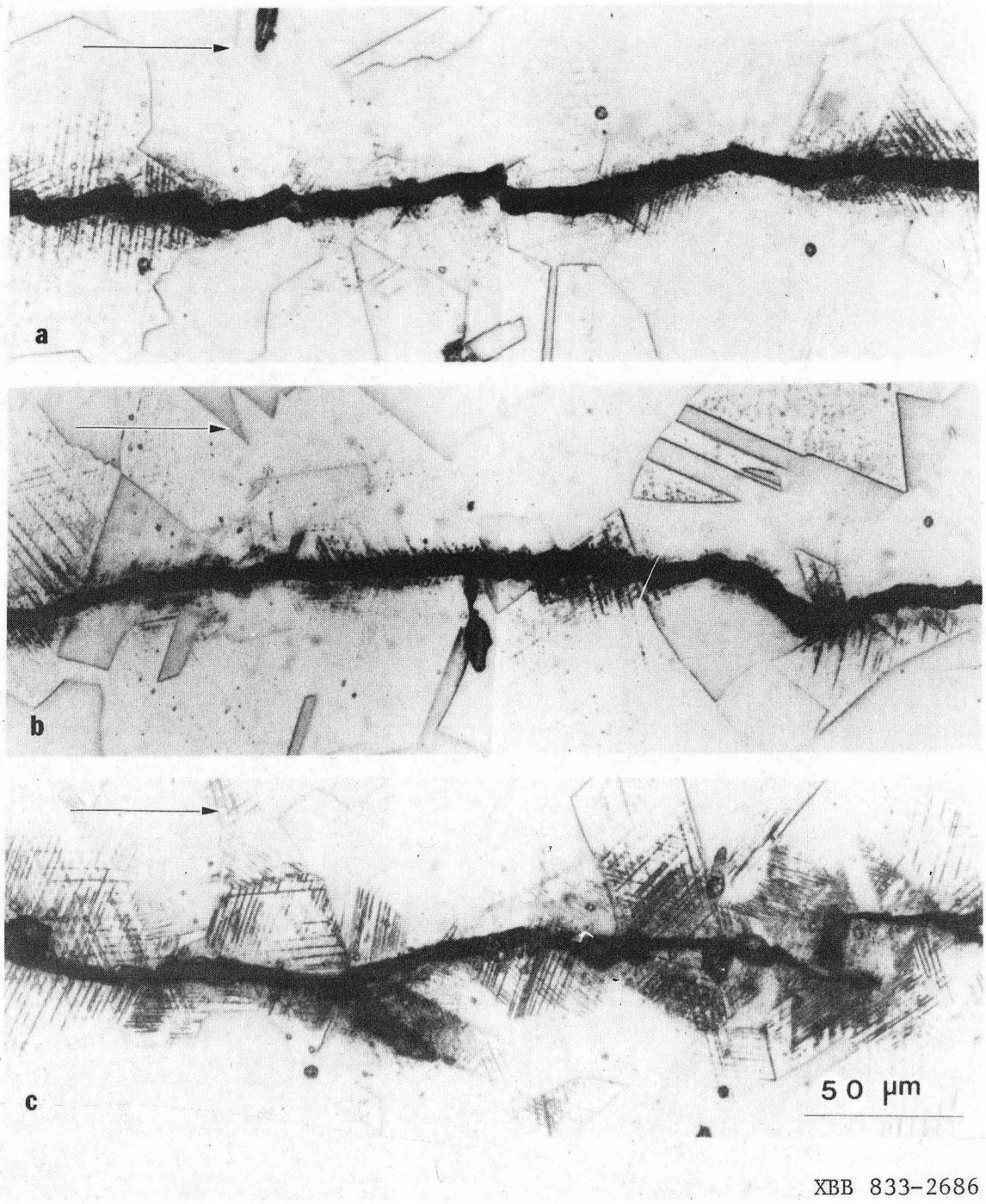

Figure 4. Crack propagation path of as-rolled plate at 4K. a) $\Delta \sim 35$ MPa m, b) $\Delta K \sim 45$ MPa m, c) $\Delta \sim 55$ MPa m.

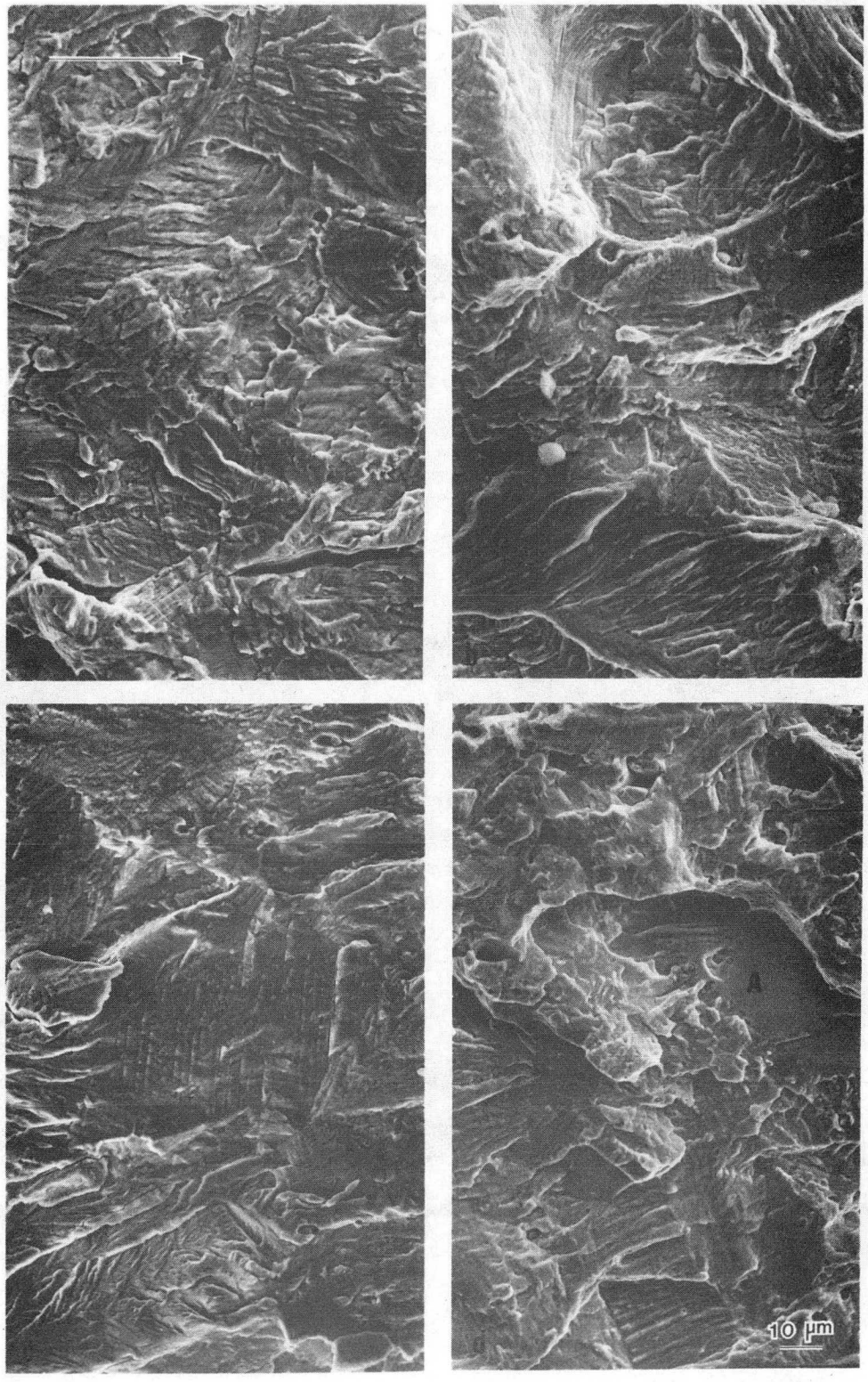

XBB 833-2689

Figure 5. Fracture surfaces after fatigue cracking at 4K. a) as-rolled $\Delta K \sim 35$ Mpa m, b) as-rolled $\Delta K \sim 45$ MPa m, c) solution treatment $\Delta K \sim 35$ MPa m, d) solution treatment $\Delta K \sim 45$ MPa m.

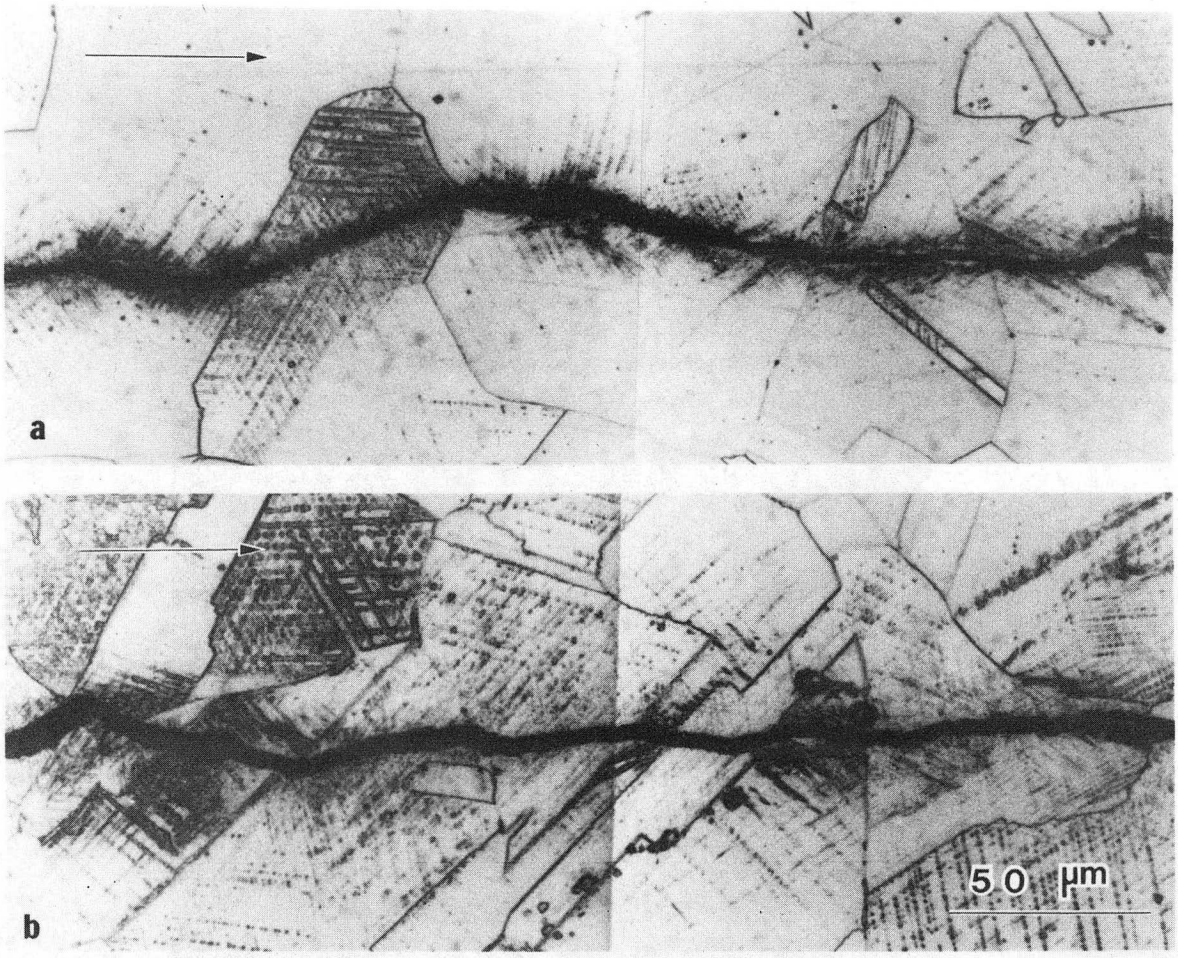

Figure 6. Crack propagation path of 304LN steel at 4K.
a) $\Delta K \sim 40$ MPa m, b) $\Delta K \sim 55$ MPa m.

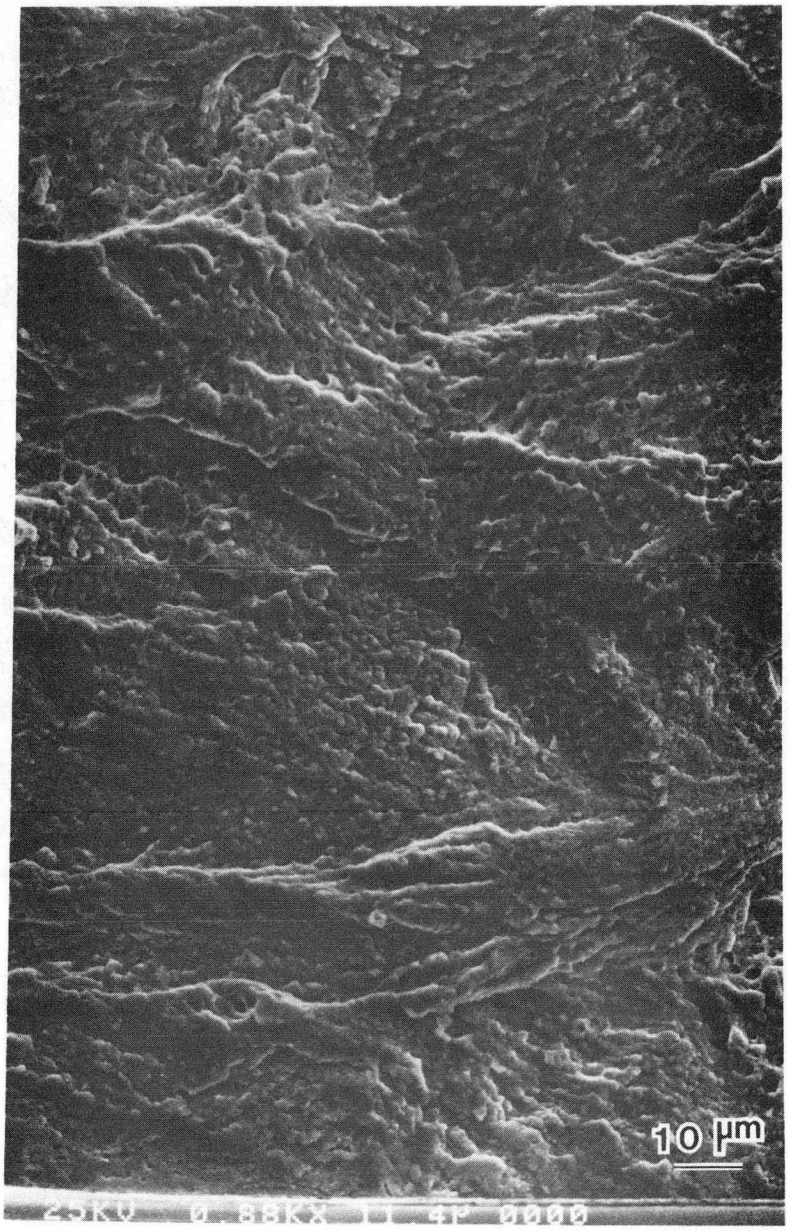

XBB 834-2497A

Figure 7. Fracture surfaces of 304LN steel after fatigue cracking at 4K, $\Delta K \sim 40$ MPa m.

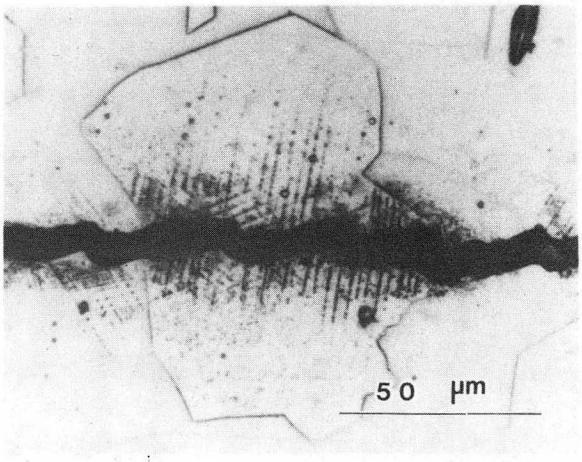

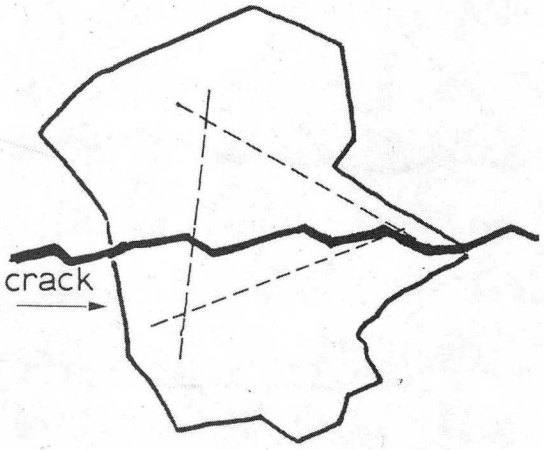

XBB 834-3545

Figure 8a. Examples of crack trace analysis of as-rolled plate after fatigue cracking at 4K. (---- = 111 slip line markings)

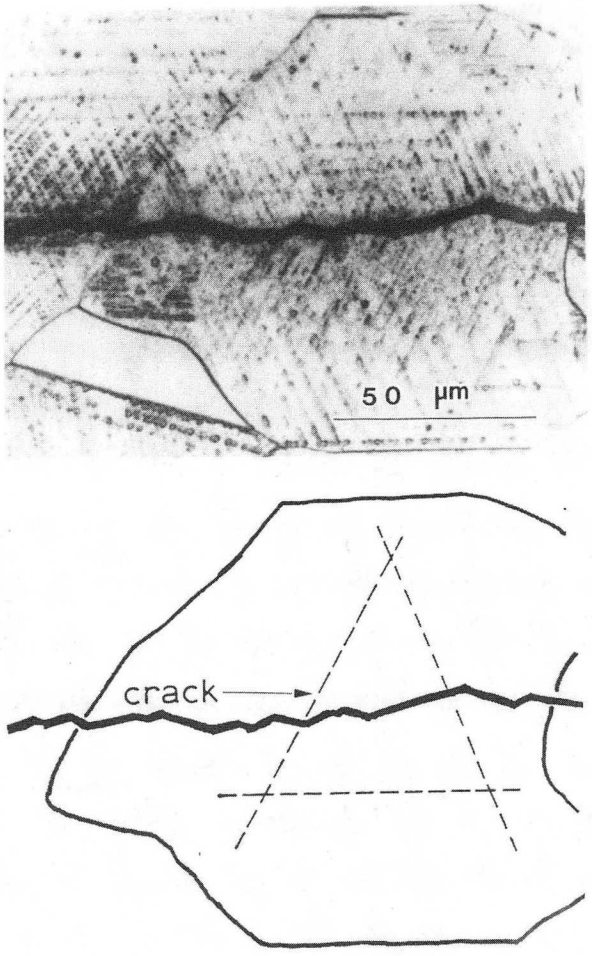

XBB 833-2681A

Figure 8b. Examples of crack trace analysis of 304LN after fatigue cracking at 4K. (---- = {111} slip line markings)

TECHNICAL INFORMATION DEPARTMENT
LAWRENCE BERKELEY LABORATORY
UNIVERSITY OF CALIFORNIA
BERKELEY, CALIFORNIA 94720